Synthesis and Conformational Analysis of Novel N(OCH_3)-linked Disaccharide Analogues

Francesco Peri,*[a] Jesús Jiménez–Barbero,[b] Víctor García–Aparicio,[b] Igor Tvaroška,[c] and Francesco Nicotra[a]

Abstract: N(OMe)-linked disaccharide analogues, isosteric to the corresponding natural disaccharides, have been synthesized by chemoselective assembly of unprotected natural monosaccharides with methyl 6-deoxy-6-methoxyamino-α-D-glucopyranoside in an aqueous environment. The coupling reactions were found to be chemo- and stereoselective affording β-(1→6) disaccharide mimics when using Glc and GlcNAc; in the case of Gal, the β-anomer was prevalent (β:α=7:1). An iterative method for the synthesis of linear N(OMe) oligosaccharide analogues was demonstrated, based on the use of an unprotected monosaccharide building block in which an oxime functionality at C-6 is converted during the synthesis into the corresponding methoxyamino group. The conformational analysis of these compounds was carried out by using NMR spectroscopy, ab initio, molecular mechanics, and molecular dynamics methods. Optimized geometries and energies of fourteen conformers for each compound have been calculated at the B3LYP/6-31G* level. Predicted conformational equilibria were compared with the results based on NMR experiments and good agreement was found. It appears that N(OMe)-linked disaccharide analogues exhibit a slightly different conformational behavior to their parent natural disaccharides.

Keywords: carbohydrates · conformation analysis · glycosylation · NMR spectroscopy

Introduction

The specific molecular recognition by protein receptors of oligosaccharides covalently attached to lipids and proteins at cell surfaces plays a key role in a number of physiological and pathological events such as cell adhesion, inflammation, metastasis, and embryonic development.[1] It is therefore not surprising that a large effort has recently been focused on the design of organic molecules that mimic the active conformation of a carbohydrate ligand, thus reproducing its biological function.

[a] Dr. F. Peri, Prof. F. Nicotra
Department of Biotechnology and Biosciences
University of Milano-Bicocca
20126 Milano (Italy)
Fax: (+39) 264483565
E-mail: francesco.peri@unimib.it

[b] Prof. J. Jiménez–Barbero, Dr. V. García–Aparicio
Departamento de Estructura y Función de Proteínas Centro de Investigaciones Biológicas
CSIC, Ramiro de Maeztu 9, 28040 Madrid (Spain)

[c] Dr. I. Tvaroška
Institute of Chemistry
Slovak Academy of Sciences
845 38 Bratislava (Slovak Republic)

Supporting information for this article is available on the WWW under http://www.chemeurj.org/ or from the author, and includes rela-

Two main strategies have been explored in the construction of oligosaccharide mimics: the substitution of the *O*-glycosidic bond with non-natural linkages or the replacement of the entire glycosidic scaffold with a new, non-carbohydrate framework bearing the required functional groups in the same spatial orientation as the parent sugar structure. The former type of mimics would ideally have increased resistance to enzymatic hydrolysis and chemical degradation, while conserving the global geometry of the native oligosaccharide.

Carbon-linked oligosaccharides are an interesting class of mimics in which a methylene group substitutes the interglycosidic oxygen. The conformational properties of *C*-glycosides have been debated.[2] Since the substitution of interglycosydic oxygen atom by the methylene group evidently results in a change in both the size and the electronic properties of the glycosidic linkages, the flexibility and the energy barriers to rotation around the inter-residual linkages are expected to change to some extent.[3] Interestingly, the conformation of *C*- and *O*-lactoses bound respectively to bovine heart galectin-1[4] and peanut lectin[5] were found to be virtually identical, while different conformers of the disaccharide and its *C*-analogue are selected and recognized by the galactose-binding protein ricin-B[2a] and by an *Escherichia coli* β-galactosidase.[6]

 DOI: 10.1002/chem.200305587

Another class of mimics, the *S*-linked oligosaccharides,[7] have several advantages over their *C*-linked counterparts: they are generally easier to prepare and have an interglycosidic sulfur atom that may act as a hydrogen bond acceptor which, as in the natural substrate, could play an important role in the binding of the ligand. These hydrolytically inert substrate analogues have been used to investigate binding and recognition events with glycosidases.[8] The *S*-linkage provides a high degree of flexibility between glycosyl units and *S*-glycosides in solution possess more low-energy conformers than their *O*-linked parent saccharides.

Finally, oligosaccharide mimics have been prepared that contain a nitrogen atom at the interglycosidic linkage[9] as well as carbopeptoids[10] or carbonucleotoids[11] in which the *O*-glycosidic bond has been replaced by a more rigid carboxyamide or phosphoramidite bond.

From a methodological point of view, the synthesis of oligosaccharides and their analogues is laborious and challenging, requiring extensive use of orthogonal protecting groups and strictly anhydrous conditions in the glycosylation reaction; for these reasons it is still far from routine, both in solution[12] and in the solid phase.[13] Synthetic strategies based on the formation of a peptide-like interglycosidic bond (carbopeptoids)[10] or based on the principle of chemoselective ligation[14] provide a powerful tool for the convergent preparation of oligosaccharide mimics. In particular, sugars bearing an aminooxy group at the anomeric position have been reacted with ketones present in a second sugar for the synthesis of complex *O*-glycosylated peptides.[15] It is also possible to link a peptide bearing an aminooxy function to the anomeric center of a free aldose in a chemoselective way, that is, without use of protecting groups.[16] It is well known that when using a reacting unit bearing a "primary" $-O-NH_2$ group, an open-chain sugar oxime is obtained,[17] but it has also been observed that the cyclic form of the sugar is restored when a peptide with a "secondary" hydroxylamino group (R–O–NH–R′) is used.[18] By following this last approach, if R and R′ were sugar units, it would be possible in principle to obtain disaccharides and, more generally, oligosaccharide mimics by working in water and avoiding the use of any activation and protection strategy. These mimics, however, differ from the natural product by the fact that two atoms (–O–N–) substitute the interglycosidic oxygen atom and they are therefore "non-isosteric" analogues.

Herein we present the synthesis and conformational analysis of a novel type of disaccharide mimic in which two monosaccharide residues are linked through a β-(1→6)-methoxyamino interglycosidic linkage.

Results

Synthesis of methoxyamino disaccharide mimics: A schematic representation of the synthesized disaccharide mimics is shown in Scheme 1. The β-(1→6)-methoxyamino interglycosidic bond allows one to exploit the chemoselective ligation procedure and afford isosteric analogues.[19] Disaccharide **1** is an isosteric mimic of the natural disaccharide gentiobiose (**7**) and **3** a mimic of allolactose (**8**). Compounds **1–6** have been assembled by chemoselective condensation of an unprotected monosaccharide bearing a methoxyamino group at C-6 and unprotected natural aldoses. The mechanism that we propose for the coupling reaction consists of the formation of an intermediate oxyiminium ion by reaction of the *N*,*O*-disubstituted hydroxylamine group with the aldehyde of the open-chain sugar (Scheme 2).[18]

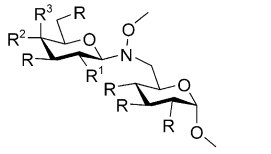

1 R=R^1=R^2=OH; R^3=H
2 R=R^1=R^2=OAc; R^3=H
3 R=R^1=R^3=OH; R^2=H
4 R=R^1=R^3=OAc; R^2=H
5 R=R^2=OH; R^3=H; R^1=NHAc
6 R=R^2=OAc; R^3=H; R^1=NHAc

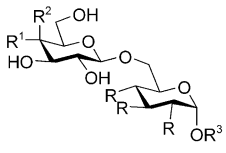

7 R=OH; R^1=OH; R^2=H; R^3=H
7a R=OH; R^1=OH; R^2=H; R^3=CH$_3$
8 R=OH; R^1=H; R^2=OH; R^3=H

Scheme 1. Amino(methoxy) disaccharide mimics **1–6** and their parent *O*-linked natural disaccharides gentiobiose (**7**) and allolactose (**8**).

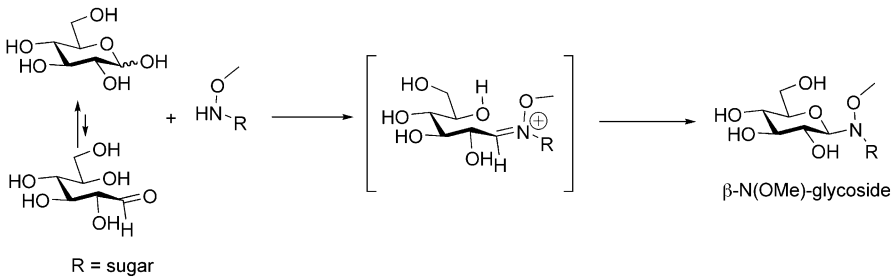

Scheme 2. Stereoselective formation of β-N(OMe)-linked glycosides via an intermediate oxyiminium ion.

Monosaccharide **13**, which has a methoxyamino group at C-6, was prepared according to the synthetic route depicted in Scheme 3.

Methyl 2,3,4-tri-*O*-acetyl-α-D-glucopyranoside (**9**) was oxidized at C-6 (Dess–Martin periodinane, CH_2Cl_2) to afford aldehyde **10** that was converted into the corresponding *O*-methyloxime **11** by treatment with *O*-methylhydroxylamine hydrochloride in pyridine. Zemplén de-*O*-acetylation with sodium methylate in methanol gave compound **12** which was reduced with $NaCNBH_3$ in glacial acetic acid to afford methyl 6-deoxy-6-methoxyamino-α-D-glucopyranoside (**13**).

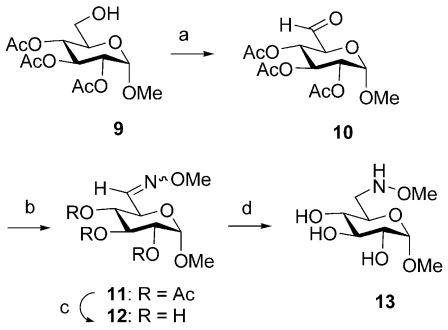

Scheme 3. a) Dess–Martin periodinane, CH_2Cl_2 (95%); b) $MeONH_2$·HCl, pyridine (75%); c) MeONa, MeOH (98%); d) $NaCNBH_3$, glacial AcOH (86%).

Compound **13** was condensed with D-glucose, D-galactose, and *N*-acetylglucosamine to afford disaccharide analogues **1**, **3**, and **5**, respectively, which were then fully acetylated (Ac_2O, pyridine, and 4-(dimethylamino)pyridine (DMAP)) leading to compounds **2**, **4**, and **6** (Scheme 4).

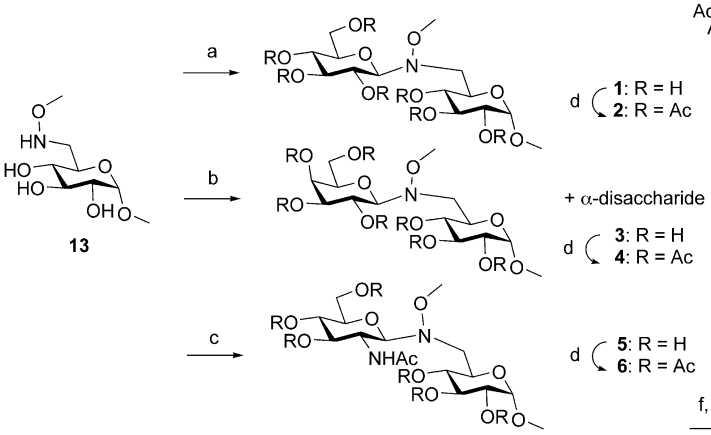

Scheme 4. a) D-Glucose, DMF/AcOH (2:1) (82%); b) D-galactose, DMF/AcOH (2:1) (75%); c) *N*-acetylglucosamine, DMF/AcOH (2:1) (80%); d) Ac_2O, pyridine, DMAP.

The coupling reactions proceeded at room temperature in 12–24 h, and were carried out either in aqueous *N*,*N*-dimethylformamide (DMF)/sodium acetate buffer (pH ≈ 4.5), water/acetic acid (1:1 v/v), or acetic acid/DMF (1:2) solvent mixtures. Reactions were never complete and after several hours a steady state was reached with a more or less constant ratio between reactants and products. Unreacted monosaccharides were recovered at the end of each reaction and recycled.

The β-disaccharide mimics **1** and **5**, which contain D-glucose and *N*-acetylglucosamine, respectively, were obtained with complete stereoselectivity. The ^{1}H NMR analysis of the D-galactose derivative **3** revealed the presence of a small amount of the α form (β:α = 7:1, as calculated from the integration ratio of the anomeric protons). Reaction of mannose with **13** gave a mixture of disaccharides in low yield (20%), the NMR analysis of which showed the presence of the pyranose ($\alpha+\beta$) and furanose ($\alpha+\beta$) forms.

The preference for the β anomer in the case of glucose, galactose, and *N*-acetylglucosamine can be explained in terms of stabilization of the β conformation of the oxyiminium intermediate (Scheme 2) through the reverse anomeric effect that is particularly relevant when a positively charged nitrogen atom is linked to the anomeric position.[20]

Iterative synthesis of methoxyamino trisaccharide mimetics: We investigated the possibility of using our chemoselective approach iteratively for the synthesis of linear oligosaccharide mimetics linked through a β-(1→6)-methoxyamino bond. To accomplish this task, we designed the monosaccharide **16** that has the two complementary functionalities required for chemoselective ligation, namely, the aldehyde and the aminomethoxy group, the latter being masked as an *O*-methyloxime.

The readily available compound **16** was coupled with **13** to afford the disaccharide **17** (Scheme 5). Reduction of the oxime group of **17** with $NaCNBH_3$ gave the disaccharide **18**,

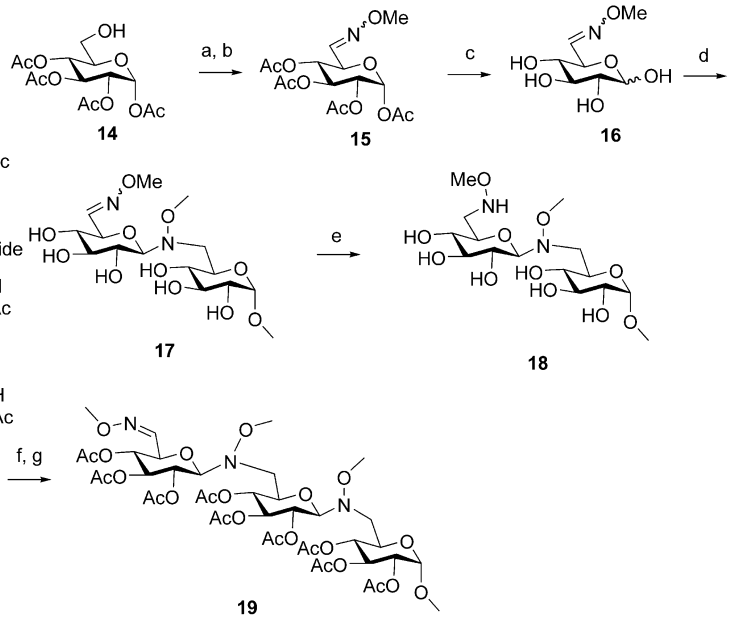

Scheme 5. a) Dess–Martin periodinane, CH_2Cl_2; b) $MeONH_2$·HCl, pyridine (75% over two steps); c) MeONa, MeOH (98%); d) **13**, DMF/AcOH (2:1) (72%); e) $NaCNBH_3$, glacial AcOH (75%); f) **16**, DMF/H_2O/AcOH (2:2:1) (43%); g) Ac_2O, pyridine, DMAP.

which has a methoxyamino group at C-6′. Chemoselective coupling with another monosaccharide, followed by treatment with Ac_2O, pyridine, and DMAP, afforded the peracetylated trisaccharide mimic **19**, which can be reduced and submitted to further elongation.

Conformational analysis: The conformational study of the disaccharide mimics with free hydroxyls and their acetylated analogues (**1**–**6**) was performed in solution. The protocol used is based on a combination of theoretical methods with ab initio and molecular mechanics and dynamics calculations, supported by experimental NMR data. Similar approaches have been demonstrated to be particularly useful

to deduce the conformational properties of other glycomimetics,[21] and also to sample the differences with respect to the natural analogues, gentiobiose (**7**) and allolactose (**8**). It has to be emphasized that these glycomimetics show a particular arrangement at the pseudoglycosidic linkage, since the nitrogen atom (which mimics the natural glycosidic oxygen) bears an additional electronegative substituent. In this context, six different staggered arrangements at angle Φ (defined as shown below) may take place, as depicted in Scheme 6, which also considers the two possible configurations at the nitrogen atom.

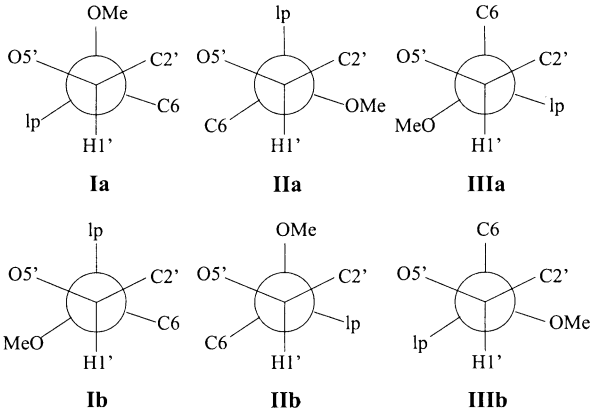

Scheme 6. Possible rotamers around Φ of compounds **1**–**6**. The different stereochemistries of the substituents at the nitrogen atom are also depicted.

Ab initio based computational analysis:

Potential energy surfaces: The available conformational space was monitored by means of a series of two-dimensional (Φ, Ψ) potential energy surfaces, each one corresponding to the one of three different starting values of ω, namely $\omega=-60°$, $\omega=60°$, and $\omega=180°$ (see Experimental Section). Figure 1 represents the B3LYP/6-31G* conformational energy maps of the *gg*, *gt*, and *tg* rotamers for the disaccharide analogue **5** calculated as a function of the torsion angles Φ and Ψ. Several energy minimum domains were found on each of these maps. For example, in the case of the *gg* rotamer (Figure 1a), four distinct low-energy regions with (Φ, Ψ) values close to (40°, 100°), (60°, 300°), (220°, 80°), and (300°, 210°), respectively, were identified. It can be seen from these three maps in Figure 1 that for the rotation about the C1−O1 linkage they all have three low-energy regions centered about $\Phi=40°$, $\Phi=240°$, and $\Phi=300°$. Three low-energy regions were found in the direction of the Ψ angle for the *gg* and *gt* rotamers. In the case of the *tg* rotamer (Figure 1c), the region centered about $\Psi=60°$ disappeared and only two regions centered around $\Psi=150°$ and $\Psi=300°$ were found in the Ψ direction. Geometries from these regions were used as the initial geometry for further optimizations of **1**, **3**, **5**, and the parent natural disaccharide methyl α-D-gentiobioside (**7a**) allowing the torsion angles Φ and Ψ to relax also. These optimizations yielded 14 local minima for each disaccharide analogue. The minima are named by a three-letter code according to the conformation around the C5–C6 linkage (GG, GT, or TG) and the number of the minimum, for example, GT1 represents the number 1 minimum ($\Phi=-72.2°$, $\Psi=-154.3°$) of the *gt* rotamer ($\omega=58.8°$).

Structure and energetics of conformers: The relative energies of the 14 minima calculated at the 6-31G* level for all methyl disaccharides in the gas phase and aqueous solution are reported in Tables 1S–4S (see Supporting Information) together with the values of Φ, Ψ, and ω torsional angles. The relevant proton–proton distances of these minima, calculated at the B3LYP/6-31G* level, are listed in Tables 5S–8S (see Supporting Information). As can be seen from Tables 1S–4S, four of the 14 calculated minima belong to the *gg* rotamer and each of the *gt* and *tg* rotamers contains five minima. Inspection of the calculated structures revealed that the counterclockwise orientation of hydroxyl groups is preferred in both monosaccharide residues. It is well known that the cooperative effect of hydrogen bonds in these arrangements favors corresponding conformations of glucopyranose and galactopyranose in the gas phase.[22] It is evident that the preferred conformations around C1′−X1′ bond (angle Φ) between the parent disaccharide and its mimics differ, *−gauche* for **7** versus *+gauche* for **1**, **3**, and **5**. The lowest-energy conformers of three N(OMe)-linked analogues **1**, **3**, and **5** lay in the low-energy domain located at $\Phi=60°$, $\Psi=100°$, whereas for the parent molecule **7a** the lowest-energy minima are at $\Phi=-71°$, $\Psi=-152°$ (*−gauche* region) and at $\Phi=-69°$, $\Psi=-90°$ (*−gauche* region), respectively. In the case of the angle Ψ, two preferred orientations, namely, *+gauche* and *trans*, were detected in the low-energy minima for all compounds.

The *gg*, *gt*, and *tg* rotamer populations calculated from the energy values together with the available experimental data are compared in Table 1. For **1**, **5**, and **7**, we found that in the gas phase at the 6-31G* level, the *gt* rotamer is the dominant species and that the stability of the hydroxymethyl rotamers is in the order $gt \gg gg \approx tg$ with the presence of the *gt* rotamer higher than 60%. This implies that the presence of the NHAc substituent at C2′ does not significantly influence the conformational equilibrium around the (1→6) linkage. The conformational preferences around the C5′−C6′ bond of the galactopyranose moiety in **3** displays similar behavior to the parent disaccharide **7a** and in a comparison to the Glc-type fragments of **1** and **5** shows a smaller dominance of the *gt* rotamer. In spite of differences in the rotamer popula-

Table 1. Rotamer populations of compounds **1**, **3**, **5**, and **7a** estimated from energies calculated at the B3LYP/6-31G* level.

	1	**3**	**5**	**7a**	Exp.(**7a**)
GG	7.7	31.4	9.6	35.1	34
GT	84.9	68.6	77.4	62.1	66
TG	7.4	0.0	13.0	2.8	0
$\langle\Phi\rangle$	27	−145	30	−145	−72
$\langle\Psi\rangle$	78	107	83	−153	−120
$\langle\omega\rangle$	100	137	109	149	-143

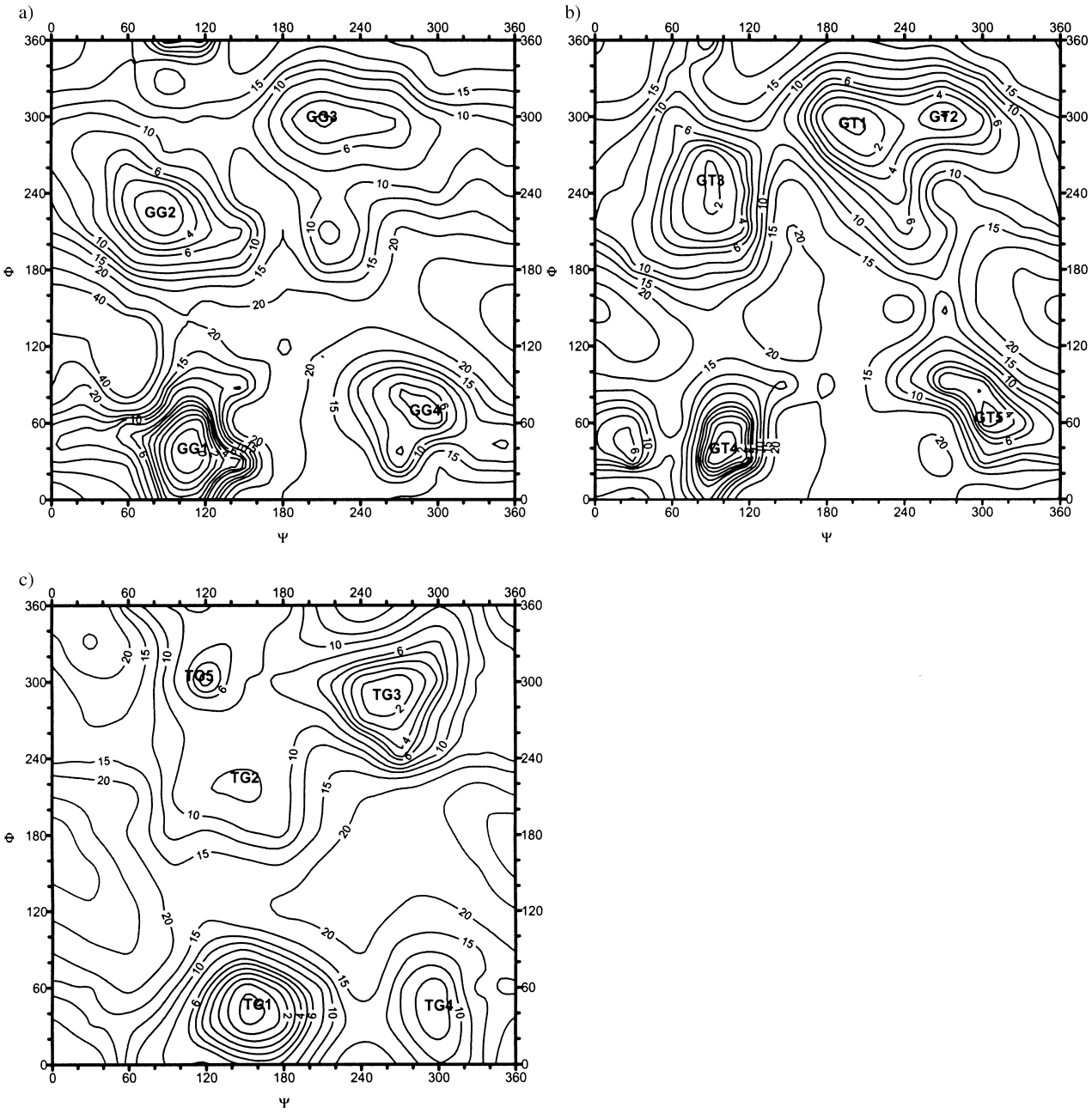

Figure 1. Relaxed conformational energy maps of compound **5** calculated at the B3LYP/6-31G* level as a function of the torsional angles Φ and Ψ, with the torsional angle ω in *gg* (a), *gt* (b), and *tg* (c) orientation. The symbols indicate local minima.

tions, the calculated average values of the torsional angles Φ and Ψ in the gas phase are very similar for all three N(OMe)-linked analogues, with $\langle\Phi\rangle$ in the range 27–63° and $\langle\Psi\rangle$ in the range 100–140°, respectively. The conformational preference around the C1′–N linkage in **1**, **3**, and **5** ($\Phi\approx +60°$) corresponds to the *gauche* orientation with respect to the C1′–O5′ and C1′–C2′ linkages and significantly differs from the "usual" conformation ($\Phi\approx -60°$) predicted by the combination of steric and stereoelectronic interaction, the *exo*-anomeric effect,[23] for β-linked oligosaccharides. However, this preference is not entirely surprising, since the similar behavior was already observed in modeling studies on amino derivatives with *S*-configuration and probably reflects steric interactions of the *N*-substituent.[24] In our compounds such a substituent is the electronegative OMe group. It appears that for the calculated lowest-energy conformers (Tables 1S–4S), the oxygen atom of the OMe moiety is in the *gauche* orientation (structures IIIa and IIb in Scheme 6) with respect to the ring oxygen. This suggests that two stereoelectronic effects influence the orientation about the C1′–N1′ bond, namely the *exo*-anomeric effect through the O5′–C1′–N1–C6 sequence and the gauche effect through the O5′–C1′–N1–O sequence. It is noteworthy that an analogous conformation about Φ with the torsional angle of $\Phi = 55.9°$ was found in the crystal structure of methyl *C*-gentiobioside.[25] This +*gauche*-type conformation has also been

detected by NMR spectroscopy for *C*-lactose as the one bound by the active site of the enzyme *E. coli* β-galactosidase.[6] It appears from our experimental data (see NMR spectroscopy section below) that solvent does not influence equilibrium in **1**, **3**, and **5**. Therefore, we did not calculate solvent effects for these compounds.

Conformational preferences around the C5–C6 bond in the parent disaccharide methyl gentiobioside (**7a**) display similar behavior to the N(OMe)-linked analogues. The *gt* rotamer is the preferred rotamer in the gas phase and the population distribution of *gg*, *gt*, and *tg* rotamers was calculated to be 35:62:3. Comparison of conformational behavior calculated by this B3LYP/6-31G* method for **1**, **5**, and **7a** show that the effect of substitution of O1′ by the N(OMe) group, going from **7** to **1** and **5**, results in a different flexibility of **1** and **5** compared to **7a** and a shift of the rotamer equilibrium towards the *gt* rotamer, which is the dominant rotamer in the N(OMe)-linked analogues **1** and **5**. It is evident that calculated conformational equilibrium around glycosidic linkages C1′–O1′ and O1′–C6 in **7a** differ from those found for **1** and **5**. For **7a**, the average values of $\langle\Phi\rangle = -145°$ and $\langle\Psi\rangle = -153°$ were calculated. The most significant difference is found for the orientation around C1–O1: $\langle\Phi\rangle = -gauche$ for **7a** versus $\langle\Phi\rangle = +gauche$ for **1** and **5**.

The conformational characteristics of gentiobiose (**7**) have been the subject of several experimental and modeling studies. The crystal structure of gentiobiose[26] is characterized by the following torsional angles: $\Phi = -58.5°$; $\Psi = -155.2°$, $\omega = -60.8°$, and $\Phi = -58.3°$; $\Psi = -156.3°$, $\omega = -61.5°$, indicating that the conformation about ω corresponds to the *gg* rotamer and the orientation about Φ is in the expected position based on the *exo*-anomeric effect. From the calculated minima, the GG3 minimum characterized by the torsional angles $\Phi = -65.6°$; $\Psi = -146.9°$ and $\omega = -62.4°$ and with the energy 1.38 kcal mol^{-1} above the lowest minimum GT2 is close to the crystal structure conformation. NMR solution data imply conformational flexibility of gentiobiose in solution reflected in a conformational equilibrium of several conformers about Φ, Ψ, and ω. The analysis of the experimental information from proton–proton and carbon–proton vicinal coupling constants and proton–proton cross-relaxation rates yielded to the presence of two major rotamers *gg* and *gt* about the C5–C6 bond, characterized by $\omega = -68.9° \pm 6.3°$ and $\omega = 79.0 \pm 3.4°$, with the estimated populations of $34 \pm 6\%$ and $66 \pm 6\%$, respectively. The calculated ratio *gg*:*gt*:*tg* = 35:62:3 and the calculated average torsional angles $\langle\omega_{GG}\rangle = -70°$ and $\langle\omega_{GT}\rangle = 87°$ are in excellent agreement with these estimates. In another experimental study,[27] the ensemble average values of vicinal heteronuclear proton–carbon coupling constants $^3J_{C,H}(\Phi) = 2.68 \pm 0.06$ Hz and $^3J_{C,H}(\Psi) = 2.36 \pm 0.06$ Hz were measured across the glycosidic linkage for gentiobiose. These values are compatible with the virtual conformation of gentiobiose characterized by the torsional angles $\langle\Phi\rangle = -145°$ and $\langle\Psi\rangle = -153°$, respectively. All this suggests that conformational equilibrium in **7a** is reasonably well represented by the calculated conformers.

Molecular mechanics and dynamics calculations: Qualitative molecular mechanics calculations were performed by using the MM2* force field with the GB/SA solvation model. The corresponding results are given in the Supporting Information. A representation of the corresponding low-energy minima is given in Figure 2, while the key geometric features that may be correlated with the NMR data are given in Table 2.

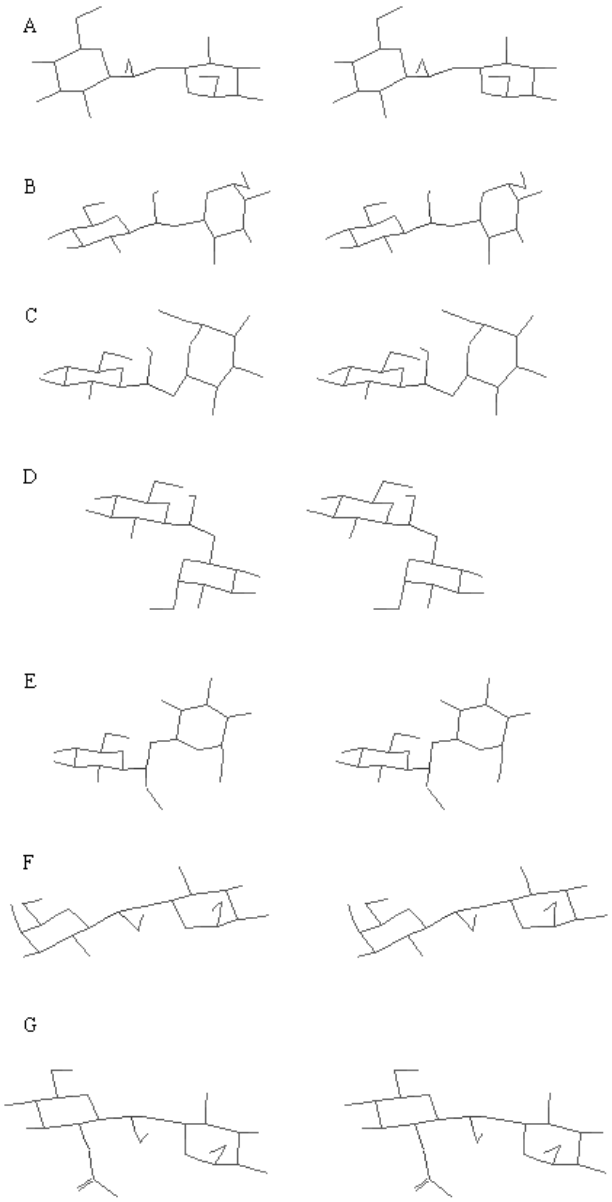

Figure 2. Stereoviews of the global and local minima of compounds **1**–**5** according to MM3* calculations. A) Conformer C (*gt* rotamer for ω angle) for compound **1**; B) conformer C (*gg* rotamer for ω angle) for compound **1**; C) conformer B for **1**; D) conformer A for **1**; E) conformer D for **1**; F) conformer C for compound **3**; G) conformer C for compound **5**. See Table 1 for the Φ and Ψ torsions of the different conformers.

NMR spectroscopy: The predictions of the ab initio and force field calculations were checked by using NMR spectroscopy. The chemical shifts in D_2O and [D_6]acetone of compounds **1**–**5** are listed in Table 9S in the Supporting Information. The assignment of the resonances was made

Table 2. Expected distances estimated from the molecular mechanics (MM) and molecular dynamics simulations (MD) for the low-energy conformers for compounds **1**–**6**.[a]

	Single conformers (Φ/Ψ) according to MM2* calculations and their relative population [%]				Average distances from MM and MD		Observed NOEs in comparison to those estimated from the calculations according to a full matrix relaxation approach		
Confomer [Φ/Ψ] →	C (54/−162)	B (54/−60)	A (54/74)	D(180/−162)					
Pop →	82–99	0–1	1–18	<0.5					
Proton pair	Distances from MM				MM	MD	NOEs from MM3 [%]	NOEs from MD [%]	Obs. NOE intensity
H1′–	**2.2**	2.9	3.6	3.7	**2.3**	2.3	7.4	7.4	strong
H1′–H6S	3.1	3.6	**2.2**	3.7	**3.0**	2.9	1.2	1.2	medium
									weak
H2′–H6S	4.4	4.8	4.9	**2.0**	4.3	4.4	0.2	0.2	very weak
H1′–H5	4.5	**2.7**	3.2	4.8	4.2	4.3	0.3	0.3	weak
H1′–Me	**3.2**/4.3	**3.2**/4.3	**3.2**/4.3	**3.2**/4.3		3.6	0.3	0.3	very weak
H2′–Me	**3.0**/4.7	**3.0**/4.7	**3.0**/4.7	**3.0**/4.7		4.2	1.3	1.3	very weak
H1′–H1	6.1	**3.0**	6.4	6.6	6.0	6.0	0.1	0.1	very weak
Coupling constants	Conformer *gg*	Conformer *gt*	Exp (**1**)	Exp (**2**)	Exp (**3**)	Exp (**4**)	Exp (**5**)	Exp (**7a**)	
H5/H6$_{proS}$	2.9	2.5	2.6	2.7	2.8	2.7	2.8	2.0	
H5/H6$_{proR}$	1.2	10.7	8.3	8.0	7.8	8.0	7.6	6.0	
gg [%]	100	0	25	29	30	29	33	66	
gt [%]	0	100	75	71	70	71	67	34	

[a] The key distances and NOEs are given in bold. Ensembled average distances together with the calculated NOEs according to a full-matrix relaxation approach in comparison with the intensities of the observed NOEs are also given. Two figures are given for H1′–Me and H2′–Me, indicating the two possible orientations of the OMe group at the nitrogen atom. The *gt* conformer was always more stable than the *gg* one, with relative populations greater than 9:1 in favor of *gt*. The ranges in populations correspond to those obtained for the different compounds. In addition, the expected *J* values (Hz) for the basic conformations around angle ω for **1**–**5**, deduced by applying the generalized Karplus equation proposed by Altona to the geometries provided by MM3 molecular mechanics calculations, are also given. The estimated populations for the different compounds are also given in comparison to those reported for gentiobiose (**7a**).

through a combination of COSY, TOCSY, 1D and 2D-NOESY/ROESY, and HSQC experiments (Figure 3 and Supporting Information).

The *J* values for the ring protons indicate that all the pyranose rings adopt the usual $^4C_1$ chair, independently of the size of the molecule and the nature of the glycosidic linkage. Although this is the usual situation, in some cases alternative chair conformations have been described for some *C*-glycosyl compounds.[28] The observed values (one small and one large) for the C5−C6 lateral chains that form part of the (1→6) linkage are in agreement with an equilibrium between the *gg* and a second conformer, which appeared to be the *gt* one (see Supporting Information for the detailed procedure of assignment).

The coupling values are given in Table 2, together with the deduced relative populations of conformers around the ω angle, calculated by applying the generalized Karplus equation proposed by Haasnoot et al.[29] to the geometries of the basic *gg* and *gt* rotamers. The obtained data are in agreement with a major presence (ca. 70%) of *gt* rotamers, in contrast with the observations for the natural compounds, gentiobiose and allolactose, for which a 34:66 equilibrium has been deduced.[30] In addition, the experimental observations indicate that the MM2* calculations slightly overestimate the experimental predominance of *gt* rotamers (experimental 70%, MM2 90%). The ab initio results are in good agreement with the observations, as they predict populations of the *gt* rotamer in the 70–85% interval. Since the stereoelectronic effects strongly affect the conformation, different chemical surroundings in the vicinity of ω should influence the conformational populations.[31] It is therefore not unexpected that the MM2 modeling data do not strictly reproduce the distribution of rotamers around ω in compounds **1**–**5** and that their actual relative populations differ from those reported for the natural compounds **7** and **8**.[30a]

NOESY and ROESY experiments (Figure 3) were also carried out to deduce the relevant conformational information of **1**–**5** around Φ and Ψ. The intensities of the observed NOEs compared to those estimated by the MM2* molecular mechanics and dynamics calculations, calculated according to a full relaxation matrix approach, are also gathered in Table 2. The observed NOE cross peaks were indeed very similar for all the compounds independent of the substitution and solvent used. The analysis of the conformational behavior of **1**–**5** was also facilitated by the stereospecific assignment of the C-6 protons. In fact, for all compounds in D_2O or [D_6]acetone, strong NOEs were observed in all cases between H-1′ and H-6*proR*, that is, the same methylene that is close to its intraresidue H-4. Therefore, the presence of this strong NOE for **1**–**6**, as shown in Table 2, pro-

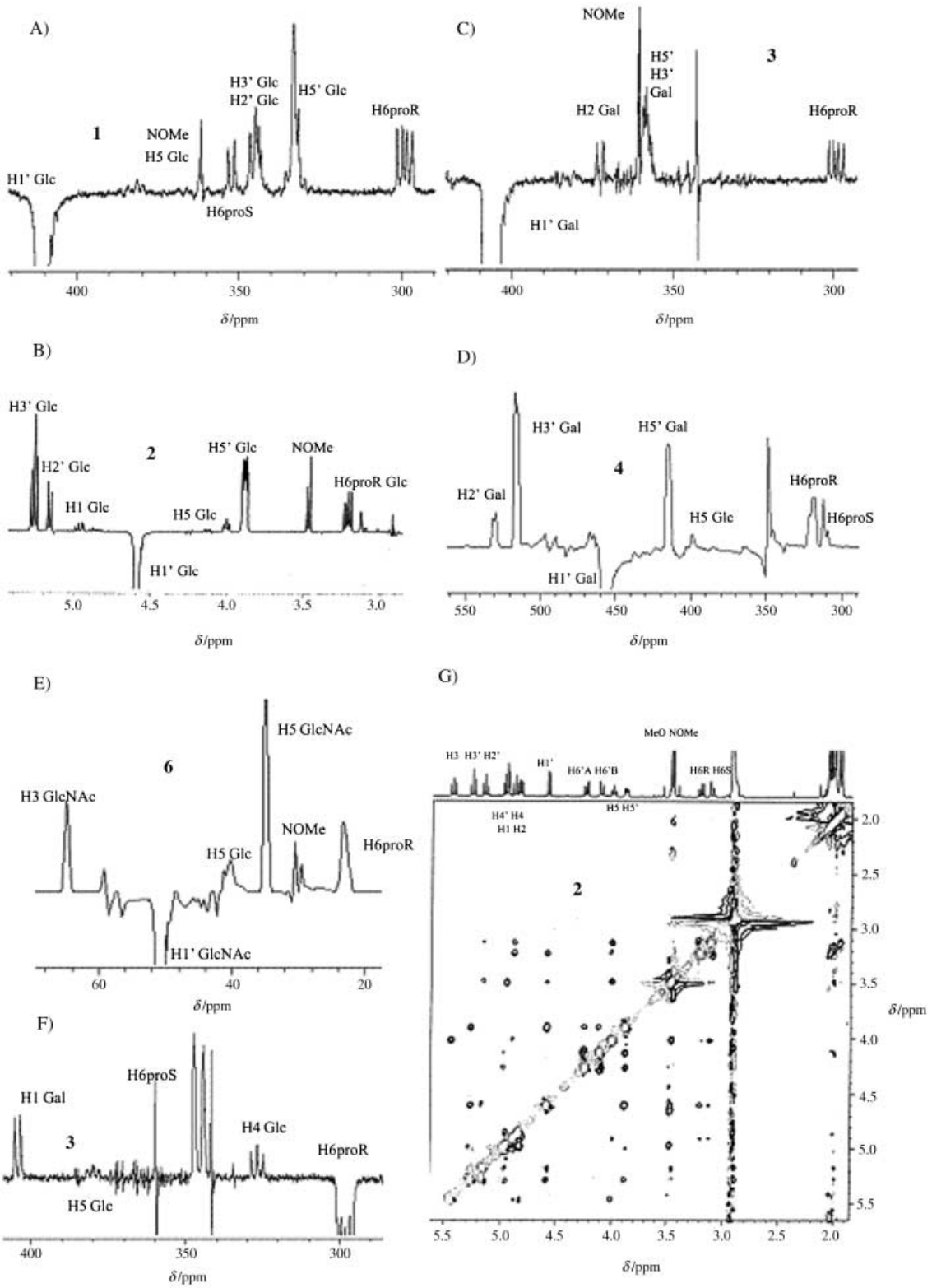

Figure 3. ^{1}H NMR 1D- and 2D-NOESY and T-ROESY data for **1**–**5** at 500 MHz and 300 K in D_2O (**1**,**3**) or $(CD_3)_2CO$ (**2**, **4**, **5**). Key cross peaks are indicated. A) 1D-NOESY spectrum obtained after inversion of H-1′ of **1**. B) 1D-NOESY spectrum obtained after inversion of H-1′ of **2**. C) 1D-NOESY spectrum obtained after inversion of H-1′ of **3**. D) Trace of the 2D-T-ROESY spectrum at the frequency of H-1′ of **4**. E) Trace of the 2D-T-ROESY spectrum at the frequency of H-1′ of **5**. F) 1D-NOESY spectrum obtained after inversion of H-6*proR* of **3**. G) 2D-T-ROESY spectrum for **3**.

vides evidence for the predominance of conformers with a C-type (*Φ*−*gauche*/*Ψanti*) orientation around the glycosidic linkages.

Nevertheless, additional cross peaks that correspond to the presence of the other conformers are also observed. For instance, the presence of very weak H1′–H1 in **2**, weak H1′–

H5 in **1**–**5**, and medium weak H1′–H-6*proS* in **1**–**5** indicate the additional participation of conformers A and B. Even the minor presence (<5%) of conformers with a (Φ+*gauche*/Ψ*anti*) orientation (D-type) is evidenced by the presence of a very weak, but detectable, H2′–H-6*proS* NOE. The absence of the H2′–H6*proR* NOE cross peak in all cases also indicates the absence of the GG4, GT5, and TG4 geometries. No major orientation of the OMe group at the nitrogen atom could be deduced, since both the H1′–Me and H2′–Me NOEs were equally weak in all compounds and solvents. Nevertheless, the magnitudes of the observed NOEs are in agreement with a major participation (>80%) of *anti*-Ψ conformers, with contributions around 5–10% of the Ψ+ and Ψ− conformers.

The agreement between the theoretical NOEs obtained from the full matrix relaxation analysis from the MM2* molecular mechanics and dynamics calculations and the observed experimental NOEs is more than satisfactory.

Therefore, after considering the *J* and NOE information, it may be considered that compounds **1**–**5** present a conformational averaging around Φ, Ψ, and ω glycosidic linkages with participation of several conformers in the conformational equilibrium with fairly small energy barriers among them, which somehow resembles that evidenced for the naturally occurring gentiobiose and allolactose, although with different populations in equilibrium, especially around ω torsion angle.[30]

Conclusion

We have demonstrated that β-(1→6)N(OMe)-linked disaccharides can be prepared by using a chemoselective approach from unprotected precursors. Yields and stereoselectivity were high in the case of compounds **1**, **3**, and **5**. This method has also been applied to the iterative preparation of a trisaccharide analogue in solution. The combination of molecular mechanics calculations and NMR experiments permits us to conclude that compounds **1**–**5**, which have an N(OMe) group at the pseudoglycosidic position, have conformational behavior similar to their natural counterparts, gentiobiose and allolactose (**7** and **8**). It seems that the difference of C–N versus C–O distances, together with the variation of bond angles (C-N-C versus C-C-C) is at the origin of this slightly different behavior. Regarding the ω angle, it has been reported that the conformational equilibrium between *gg* and *gt* rotamers in **7** is strongly biased by solvation effects.[30] Since the stereoelectronic effects for the natural compounds and the N(OMe)-linked analogues must obviously be rather different at this torsion angle, these properties must be at the origin of the observed conformational differences. Indeed, the ab initio calculations performed at the B3LYP/6-31G* level of theory reproduce the conformational behavior of **1**–**5** in solution reasonably well. Nevertheless, all the conformations sampled by the natural compounds are also accessible for these glycomimetics. On the other hand, the estimation of relatively low energy barriers between the different conformational regions of these analogues, indicate that conformers different to the major one existing in solution may be bound by the binding site of proteins without major energy conflicts.

Experimental Section

General methods: All solvents were dried over molecular sieves (Fluka) for at least 24 h prior to use. When dry conditions were required, the reactions were performed under an argon atmosphere. Thin-layer chromatography (TLC) was performed on silica gel 60 F_{254} plates (Merck) with detection with UV light when possible, or charring with a solution containing concentrated H_2SO_4/EtOH/H_2O (5:45:45) followed by heating at 180 °C. Column flash chromatography was performed on silica gel 230–400 mesh (Merck). The boiling range of petroleum ether used as eluent in column chromatography is 40–60 °C. Usual workup refers to dilution with an organic solvent, washing with water to neutrality (pH test paper), drying with Na_2SO_4, filtration, and evaporation under reduced pressure. Routine ^{1}H and ^{13}C NMR spectra were recorded at 400 MHz on a Varian Mercury instrument with $CDCl_3$ as solvent at 300 K unless otherwise stated. Chemical shifts are reported in ppm downfield from TMS as an internal standard. Aromatic signals and methyl signals of peracetylated sugars are omitted in ^{1}H spectra; carbonyl and methyl carbons of peracetylated sugars are omitted in ^{13}C spectra. Mass spectra were recorded on a MALDI2 Kompakt Kratos instrument with gentisic acid (DHB) as matrix. Optical rotations were measured at ambient temperature (22±2 °C) on a Perkin–Elmer 241 polarimeter.

Model and computational procedures: The relative orientation of two contiguous (1→6)-linked monosaccharide residues is described by the three torsion angles Φ, Ψ, and ω, where $\Phi = \Theta$(O5–C1–X–C6); $\Psi = \Theta$(C1–X–C6–C5); $\omega = \Theta$(X–C6–C5–O5), in **1**–**6**, X represents N and in **7** and O1′ in **8**, respectively. Available conformational space was monitored by means of a series of two-dimensional (Φ, Ψ) potential energy surfaces, each one corresponding to one of three different starting values of ω, namely $\omega = -60°$, $\omega = 60°$, and $\omega = 180°$. These ω values characterize the *gauche–gauche* (*gg*), *gauche–trans* (*gt*), and *trans–gauche* (*tg*) rotamers around the C5–C6 linkage, respectively. Torsional angles Φ and Ψ were varied by 30° increments, within the 0–360° range. During the optimization, all geometrical parameters including ω were optimized. The calculations were carried out by using the Jaguar program.[32] Optimization of the geometry was performed by using the B3LYP density functional method[33] with the 6-31G* basis set. The geometries of all local minima identified on the maps were then fully optimized with no constraints on the Φ, Ψ, and ω torsion angles. The single-point energy of all minima determined at the B3LYP/6-31G* level were calculated by using the B3LYP/6-311++G** basis set. The effect of solvent on conformational equilibrium has been investigated by using a procedure implemented in the Jaguar program at the B3LYP/6-31G* level.

NMR spectroscopy: 500 MHz ^{1}H NMR spectra were recorded at 300 K in D_2O (**1**, **3**) or [D_6]acetone (**2**, **4**, **5b**) on a Bruker DRX 500 spectrometer. Concentrations of approximately 3 mM were used. Chemical shifts are reported in ppm, using external tetramethylsilane (TMS) or 2,2-dimethyl-2-silapentane-5-sulfonate sodium salt (DSS, 0 ppm) as reference. The 2D-TOCSY experiment (70-ms mixing time) was performed with a data matrix of 256×2 K to digitize a spectral width of 3000 Hz. Four scans were used per increment with a relaxation delay of 2 s. 2D-NOESY (300, 400, and 500 ms) and 2D-T-ROESY experiments (300 and 400 ms) used the standard sequences. One-dimensional-selective NOE spectra were acquired by using the double-echo sequence proposed by Shaka and coworkers[34] at five different mixing times (200, 400, 600, 800, and 1000 ms). NOESY back calculations were performed as described. All the theoretical NOE calculations were automatically performed by a home-made program, which is available from the authors upon request.[35]

Methyl 2,3,4-tri-*O*-acetyl-α-D-gluco-hexodialdo-1,5-pyranoside-6-*O*-methyloxime (11): Dess–Martin periodinane (2.98 g, 7.03 mmol) was added to a solution of **9** (1.5 g, 4.69 mmol) in dry dichloromethane (20 mL) under an argon atmosphere. The solution was stirred for 1 h. After dilution with dichloromethane (30 mL), a saturated solution of sodium bicarbonate and sodium thiosulfate (40 mL) was added and the mixture was vigo-

rously stirred for 10 min. After usual workup compound **10** was recovered as a colorless oil (1.42 g, 95%) and used without further purification in the following reaction step. *O*-Methylhydroxylamine hydrochloride (587 mg, 7.03 mmol) was added to a solution of **10** in dry pyridine (15 mL) and the mixture was stirred for 1 h. The solvent was then evaporated and chromatography of the residue on silica gel with petroleum ether/ethyl acetate (60:40) gave **11** (1.16 g, 75%). $[\alpha]_D = +33.6$ ($c = 1$ in methanol); ^{1}H NMR: $\delta = 7.23$ (d, 1H, $J_{5,6} = 7.1$ Hz; H-6), 5.51 (t, 1H, $J_{2,3} = J_{3,4} = 10.1$ Hz; H-3), 5.02 (t, 1H, $J_{3,4} = J_{4,5} = 10.1$ Hz; H-4), 4.94 (d, 1H, $J_{1,2} = 3.6$ Hz; H-1), 4.86 (dd, 1H, $J_{1,2}$ 3.6 Hz, $J_{2,3} = 10.2$ Hz; H-2), 4.30 (dd, 1H, $J_{5,6} = 7.1$ Hz, $J_{4,5} = 10.1$ Hz; H-5), 3.82 (s, 3H; N–OCH_3), 3.41 ppm (s, 3H; OCH_3); ^{13}C NMR: $\delta = 145.7$, 97.06, 71.16, 70.30, 69.62, 67.61, 62.40, 56.05 ppm; MALDI-MS: m/z: 371.7 $[M+H+Na]^+$, 387.8 $[M+H+K]^+$; elemental analysis calcd (%) for $C_{14}H_{21}NO_9$: C 48.41, H 6.09, N 4.03; found: C 48.78, H 5.87, N 4.40.

Methyl α-D-gluco-hexodialdo-1,5-pyranoside-6-*O*-methyloxime (12): A catalytic amount of metallic Na was added to a solution of **11** (1.0 g, 2.88 mmol) in dry methanol (30 mL) under an argon atmosphere and the mixture was stirred for 4 h. Amberlite IRA-120 H^+ resin was then added until a neutral pH was reached. The mixture was then filtered to remove resin and concentrated to dryness to afford pure compound **12** (623 mg, 98%). $[\alpha]_D = +23.6$ ($c = 1$ in methanol); ^{1}H NMR: $\delta = 7.39$ (d, 1H, $J_{5,6} = 6.1$ Hz; H-6), 4.77 (d, 1H, $J_{1,2} = 3.6$ Hz; H-1), 4.13 (dd, 1H, $J_{5,6} = 6.1$ Hz, $J_{4,5} = 9.8$ Hz; H-5), 3.88 (s, 3H; N–OCH_3), 3.77 (t, 1H, $J_{2,3} = J_{3,4} = 9.2$ Hz; H-3), 3.55 (dd, 1H, $J_{1,2} = 3.6$ Hz, $J_{2,3} = 9.2$ Hz; H-2), 3.51 (t, 1H, $J_{3,4} = J_{4,5} = 9.5$ Hz; H-4), 3.43 ppm (s, 3H; OCH_3); ^{13}C NMR: $\delta = 147.96$, 99.81, 73.63, 72.35, 71.78, 69.41, 62.26, 55.91 ppm; MALDI-MS: m/z: 244.2 $[M+Na]^+$, 259.9 $[M+K]^+$; elemental analysis calcd (%) for $C_8H_{15}NO_6$: C 43.44, H 6.83, N 6.33; found: C 43.58, H 6.41, N 6.05.

Methyl 6-deoxy-6-methoxyamino-α-D-glucopyranoside (13): $NaCNBH_3$ (154 mg, 2.44 mmol) was added to a solution of **12** (360 mg, 1.63 mmol) in glacial AcOH (10 mL) under an argon atmosphere. The mixture was stirred for 1 h, and the solvent was then evaporated in vacuo. The residue was purified by chromatography on silica gel with ethyl acetate/methanol (90:10) to give **13** (313 mg, 86%). $[\alpha]_D = +25.5$ ($c = 1$ in methanol); ^{1}H NMR (CD_3OD): $\delta = 4.88$ (br s, 1H; NH), 4.66 (d, 1H, $J_{1,2} = 3.7$ Hz; H-1), 3.76 (m, 1H; H-5), 3.59 (t, 1H, $J_{2,3} = J_{3,4} = 9.4$ Hz; H-3), 3.51 (s, 3H; N–OCH_3), 3.41 (s, 3H; OCH_3), 3.39 (dd, 1H; H-6b), 3.36 (dd, 1H, $J_{1,2} = 3.7$ Hz, $J_{2,3} = 9.4$ Hz; H-2), 3.13 (dd, 1H, $J_{3,4} = 8.8$ Hz, $J_{4,5} = 9.8$ Hz; H-4), 2.82 ppm (dd, 1H, $J_{5,6a} = 8.6$ Hz, $J_{6a,6b} = 13.4$ Hz; H-6a); ^{13}C NMR (CD_3OD): $\delta = 102.3$, 76.4, 75.6, 74.9, 69.8, 62.5, 56.9, 55.0 ppm; MALDI-MS: m/z: 246.5 $[M+Na]^+$, 262.6 $[M+K]^+$; elemental analysis calcd (%) for $C_8H_{17}NO_6$: C 43.04, H 7.68, N 6.27; found: C 42.68, H 7.44, N 6.90.

Standard procedure for disaccharide formation: Reducing sugars (0.54 mmol) were added to a solution of **13** (100 mg, 0.45 mmol) in the appropriate solvent mixture (5 mL), and the mixture was stirred for 24 h. The solvents were then evaporated in vacuo and chromatography of the residue on silica gel gave pure disaccharides. To obtain peracetylated disaccharides, compounds **1**, **3**, and **5** (100 mg) were dissolved in Ac_2O/pyridine (1:2, 5 mL) and a catalytic amount of *N*,*N*-dimethylaminopyridine was added. The mixture was stirred 4 h and then diluted with methanol to destroy the excess of Ac_2O, solvents were evaporated in vacuo and chromatography of the residue on silica gel afforded peracetylated disaccharides.

Methyl 6-deoxy-6-methoxyamino-6-*N*-(β-D-glucopyranosyl)-α-D-glucopyranoside (1): Standard procedure for disaccharide formation was used: Compound **13** (100 mg, 0.45 mmol) was treated with D-glucose (97 mg, 0.54 mmol) in a mixture DMF/0.1 M aqueous sodium acetate buffer pH 4.5 (1:1) as solvent. Column chromatography of the reaction crude with AcOEt/MeOH/water (70:20:10) afforded **1** (140 mg, 82%). $[\alpha]_D = +63.6$ ($c = 1.5$ in H_2O); ^{1}H NMR (500 MHz, D_2O): $\delta = 4.78$ (d, 1H, $J_{1,2} = 4.1$ Hz; H-1), 4.15 (d, 1H, $J_{1',2'} = 9.3$ Hz; H-1′), 3.89 (dd, 1H, $J_{5',6'b} = 5.1$ Hz, $J_{6'a,6'b} = 12.4$ Hz; H-6′b), 3.81 (dd, 1H, $J_{2,3} = 9.7$ Hz, $J_{3,4} = 8.9$ Hz; H-3), 3.72 (dd, 1H, $J_{5',6'a} = 2.6$ Hz, $J_{6'a,6'b} = 12.4$ Hz; H-6′a), 3.65 (m, 1H; H-5), 3.55 (dd, 1H, $J_{1,2} = 4.1$ Hz, $J_{2,3} = 9.7$ Hz; H-2), 3.55 (t, 1H, $J_{2',3'} = J_{3',4'} = 9.3$ Hz; H-3′), 3.51 (dd, 1H, $J_{6a,6b} = 14.7$ Hz; H-6b), 3.50 (t, 1H, $J_{1',2'} = J_{2',3'} = 9.3$ Hz; H-2′), 3.49 (s, 3H; N–OCH_3), 3.46 (s, 3H; OCH_3), 3.40 (ddd, 1H, $J_{5',6'a} = 2.6$ Hz, $J_{5',6'b} = 5.1$ Hz, $J_{4',5'} = 9.7$ Hz; H-5′), 3.37 (dd, 1H, $J_{3',4'} = 9.3$ Hz, $J_{4',5'} = 9.7$ Hz; H-4′), 3.31 (t, 1H, $J_{3,4} = J_{4,5}$ 9.6 Hz; H-4), 3.01 ppm (dd, 1H, $J_{5,6a}$ 8.2 Hz, $J_{6a,6b}$ 14.7 Hz; H-6a); ^{13}C NMR: $\delta = 99.8$, 93.6, 77.6, 77.3, 72.9, 71.9, 71.2, 70.06, 70.05, 69.6, 62.6, 61.1, 56.4, 55.3 ppm; MALDI-MS: m/z: 408.8 $[M+Na]^+$, 424.4 $[M+K]^+$; elemental analysis calcd (%) for $C_{14}H_{27}NO_{11}$: C 43.63, H 7.06, N 3.63; found: C 44.51, H 6.88, N 3.77.

Methyl 2,3,4-tri-*O*-acetyl-6-deoxy-6-methoxyamino-6-*N*-(2′,3′,4′,6′-tetra-*O*-acetyl-β-D-glucopyranosyl)-α-D-glucopyranoside (2): $[\alpha]_D = +69.4$ ($c = 0.7$ in chloroform); ^{1}H NMR (500 MHz, [D$_6$]acetone): $\delta = 5.45$ (t, 1H, $J_{2,3} = J_{3,4} = 9.8$ Hz; H-3), 5.28 (t, 1H, $J_{2',3'} = J_{3',4'} = 9.3$ Hz; H-3′), 5.16 (t, 1H, $J_{1',2'} = J_{2',3'} = 9.8$ Hz; H-2′), 4.99 (dd, 1H, $J_{3',4'} = 9.3$ Hz , $J_{4',5'} = 9.5$ Hz; H-4′), 4.95 (d, 1H, $J_{1,2} = 5.0$ Hz; H-1), 4.89 (t, 1H, $J_{3,4} = J_{4,5} = 9.8$ Hz; H-4), 4.84 (dd, 1H, $J_{1,2} = 5.0$ Hz, $J_{2,3} = 9.8$ Hz; H-2), 4.59 (d, 1H, $J_{1',2'} = 9.0$ Hz; H-1′), 4.26 (dd, 1H, $J_{5',6'b} = 5.1$ Hz, $J_{6'a,6'b} = 12.2$ Hz; H-6′b), 4.12 (dd, 1H, $J_{5',6'a} = 2.4$ Hz, $J_{6'a,6'b} = 12.2$ Hz; H-6′a), 4.01 (m, 1H; H-5), 3.85 (ddd, 1H, $J_{5',6'a} = 2.4$ Hz, $J_{5',6'b} = 5.1$, $J_{4',5'} = 9.5$ Hz; H-5′), 3.45 (s, 3H; N–OCH_3), 3.44 (s, 3H; OCH_3), 3.21 (dd, 1H, $J_{5,6b} = 8.1$ Hz, $J_{6a,6b} = 14.6$ Hz; H-6b), 3.11 ppm (dd, 1H, $J_{5,6a} = 2.2$ Hz, $J_{6a,6b} = 14.6$ Hz; H-6a); ^{13}C NMR: $\delta = 96.8$, 92.4, 74.5, 73.9, 71.1, 70.8, 70.3, 69.0, 68.8, 68.6, 62.5, 62.0, 55.8, 53.9 ppm; MALDI-MS: m/z: 703.0 $[M+H+Na]^+$, 718.9 $[M+H+K]^+$; elemental analysis calcd (%) for $C_{28}H_{41}NO_{18}$: C 49.48, H 6.08, N 2.06; found: C 50.15, H 6.78, N 2.71.

Methyl 6-deoxy-6-methoxyamino-6-*N*-(β-D-galactopyranosyl)-α-D-glucopyranoside (3): Standard procedure for disaccharide formation was used: Compound **13** (100 mg, 0.45 mmol) was treated with D-galactose (97 mg, 0.54 mmol) in a mixture DMF/AcOH (2:1) as solvent. Column chromatography of reaction crude with AcOEt/MeOH/water (70:20:10) afforded a mixture of α- and β-disaccharides (148 mg, 85%) (β/α ratio of about 7 as determined by the integration of H-1′ protons in ^{1}H NMR). Further chromatographic purification of the mixture with the same eluent afforded pure **3** (128 mg, 75%). $[\alpha]_D = +74.7$ ($c = 1$ in H_2O); ^{1}H NMR (500 MHz, D_2O): $\delta = 4.75$ (d, 1H, $J_{1,2} = 3.8$ Hz; H-1), 4.05 (d, 1H, $J_{1',2'} = 9.1$ Hz; H-1′), 3.89 (dd, 1H, $J_{3',4'} = 3.4$ Hz , $J_{4',5'} = 0.6$ Hz; H-4′), 3.76 (dd, 1H, $J_{3,4} = 8.2$ Hz, $J_{2,3} = 9.7$ Hz; H-3), 3.75 (m, 1H; H-5′), 3.74 (m, 1H; H-6′b), 3.70 (m, 1H; H-5), 3.69 (m, 1H; H-6′a), 3.68 (dd, 1H, $J_{3',4'} = 3.4$ Hz, $J_{2',3'} = 9.4$ Hz ; H-3′), 3.58 (t, 1H, $J_{1',2'} = J_{2',3'} = 9.4$ Hz; H-2′), 3.52 (dd, 1H, $J_{1,2} = 3.8$ Hz, $J_{2,3} = 9.7$ Hz; H-2), 3.49 (dd, 1H, $J_{5,6b} = 3.7$ Hz, $J_{6a,6b} = 14.4$ Hz; H-6b), 3.48 (s, 3H; N–OCH_3), 3.45 (s, 3H; OCH_3), 3.30 (dd, 1H, $J_{3,4} = 8.2$ Hz, $J_{4,5} = 9.7$ Hz; H-4), 3.02 ppm (dd, 1H, $J_{5,6a} = 6.7$ Hz, $J_{6a,6b} = 14.4$ Hz; H-6a); MALDI-MS: m/z: 408.4 $[M+Na]^+$, 424.6 $[M+K]^+$; elemental analysis calcd (%) for: C 43.63, H 7.06, N 3.63; found: C 43.97, H 7.45, N 3.12.

Methyl 2,3,4-tri-*O*-acetyl-6-deoxy-6-methoxyamino-6-*N*-(2′,3′,4′,6′-tetra-*O*-acetyl-β-D-galactopyranosyl)-α-D-glucopyranoside (4): $[\alpha]_D = +68.6$ ($c = 0.7$ in chloroform); ^{1}H NMR (500 MHz, [D$_6$]acetone): $\delta = 5.47$ (t, 1H, $J_{2,3} = J_{3,4} = 9.8$ Hz; H-3), 5.39 (dd, 1H, $J_{3',4'} = 3.1$ Hz , $J_{4',5'} = 1.1$ Hz; H-4′), 5.29 (dd, 1H, $J_{1',2'} = 9.5$ Hz, $J_{2',3'} = 9.9$ Hz; H-2′), 5.18 (dd, 1H, $J_{3',4'} = 3.1$ Hz, $J_{2',3'} = 9.9$ Hz; H-3′), 4.97 (d, 1H, $J_{1,2} = 5.0$ Hz; H-1), 4.86 (dd, 1H, $J_{1,2} = 5.0$ Hz, $J_{2,3} = 9.7$ Hz; H-2), 4.86 (t, 1H, $J_{3,4} = J_{4,5} = 9.8$ Hz; H-4), 4.58 (d, 1H, $J_{1',2'} = 9.5$ Hz; H-1′), 4.19 (m, 1H; H-6′b), 4.15 (m, 1H; H-6′a), 4.02 (m, 1H; H-5), 3.85 (dt, 1H, $J_{4',5'} = 1.1$ Hz, $J_{5',6'a} = J_{5',6'b} = 7.0$ Hz; H-5′), 3.49 (s, 3H; OCH_3), 3.48 (s, 3H; N–OCH_3), 3.19 (dd, 1H, $J_{5,6b} = 8.3$ Hz, $J_{6a,6b} = 14.8$ Hz; H-6b), 3.10 ppm (dd, 1H, $J_{5,6a} = 2.2$ Hz, $J_{6a,6b} = 14.8$ Hz; H-6a); ^{13}C NMR: $\delta = 96.8$, 92.8, 72.6, 72.5, 71.1, 70.8, 70.3, 69.1, 67.4, 66.3, 62.0, 61.5, 55.8, 54.0 ppm; MALDI-MS: m/z: 702.8 $[M+Na]^+$, 718.2 $[M+K]^+$; elemental analysis calcd (%) for $C_{28}H_{41}NO_{18}$ C 49.48, H 6.08, N 2.06; found: C 48.85, H 6.33, N 1.91.

Methyl 6-deoxy-6-methoxyamino-6-*N*-(2-acetamido-2-deoxy-β-D-glucopyranosyl)-α-D-glucopyranoside (5): Standard procedure for disaccharide formation was used: Compound **13** (100 mg, 0.45 mmol) was reacted with D-*N*-acetylglucosamine (120 mg, 0.54 mmol) in a mixture DMF/AcOH/water (2:2:1). Column chromatography of reaction crude with AcOEt/MeOH/water (70:20:10) afforded **5** (184 mg, 80%). $[\alpha]_D = +64.8$ ($c = 0.5$ in H_2O); ^{1}H NMR (D_2O): $\delta = 4.62$ (d, 1H, $J_{1,2} = 3.7$ Hz; H-1), 4.09 (d, 1H, $J_{1',2'} = 9.3$ Hz; H-1′), 3.71 (br t, 1H, $J_{1',2'} = J_{2',3'} = 9.3$ Hz; H-2′), 3.70 (m, 1H; H-6′a), 3.61 (m, 1H; H-5), 3.54 (dd, 1H, $J_{5',6'b} = 4.8$ Hz, $J_{6'a,6'b} = 12.7$ Hz; H-6′b), 3.46 (t, 1H, $J_{2,3} = J_{3,4} = 8.9$ Hz; H-3), 3.34 (dd, 1H, $J_{1,2} = 3.7$ Hz, $J_{2,3} = 8.9$ Hz; H-2), 3.36 (m, 1H; H-6b), 3.35–3.21 (m, 3H; H-3′, H-4′, H-5′), 3.35 (s, 3H; N–OCH_3), 3.26 (s, 3H; OCH_3), 3.21 (t, 1H, $J_{3,4} = J_{4,5} = 9.0$ Hz; H-4), 2.82 ppm (dd, 1H, $J_{5,6a} = 8.4$ Hz, $J_{6a,6b} = 14.6$ Hz; H-6a); ^{13}C NMR (D_2O): $\delta = 173.8$,?99.5, 92.2, 77.7, 75.8, 73.1, 72.1, 71.3, 70.4, 69.8, 61.7, 61.1, 55.9, 52.8 ppm; MALDI-MS: m/z: 449.7 $[M+Na]^+$, 465.6 $[M+K]^+$; elemental analysis calcd (%) for $C_{16}H_{30}N_2O_{11}$: C 45.07, H 7.09, N 6.57; found: C 46.21, H 6.98, N 7.07.

Methyl 2,3,4-tri-*O*-acetyl-6-deoxy-6-methoxyamino-6-*N*-(3′,4′,6′-tetra-*O*-acetyl-2-acetamido-2-deoxy-β-D-glucopyranosyl)-α-D-glucopyranoside (6): $[\alpha]_D = +68.4$ ($c = 0.5$ in chloroform); ^{1}H NMR (500 MHz, [D$_6$]acetone): $\delta = 5.47$ (t, 1H, $J_{2,3} = J_{3,4} = 9.9$ Hz; H-3), 5.25 (dd, 1H, $J_{2',3'} = 9.0$ Hz, $J_{3',4'} = 9.3$ Hz; H-3′), 4.96 (dd, 1H, $J_{3',4'} = 9.3$ Hz , $J_{4',5'} = 9.6$ Hz; H-4′), 4.92 (d, 1H, $J_{1,2} = 5.1$ Hz; H-1), 4.83 (dd, 1H, $J_{1,2} = 5.1$ Hz, $J_{2,3} = 9.9$ Hz; H-2), 4.81 (t, 1H, $J_{3,4} = J_{4,5} = 9.9$ Hz; H-4), 4.53 (d, 1H, $J_{1',2'} = 9.0$ Hz; H-1′), 4.25 (m, 1H; H-6′b), 4.16 (dd, 1H, $J_{1',2'} = 9.0$ Hz, $J_{2',3'} = 10.1$ Hz; H-2′), 4.11 (m, 1H; H-6′a), 4.02 (m, 1H; H-5), 3.78 (m, 1H; H-5′), 3.52 (s, 3H; OCH$_3$), 3.49 (s, 3H; N–OCH$_3$), 3.20 (m, 1H; H-6b), 3.14 ppm (m, 1H; H-6a); ^{13}C NMR: $\delta = 96.98$, 94.22, 75.07, 74.11, 71.19, 70.52, 70.46, 68.73, 68.16, 62.75, 56.03, 51.27, 23.69 ppm; MALDI-MS: m/z: 701.4 $[M+Na]^+$, 717.6 $[M+K]^+$; elemental analysis calcd (%) for $C_{28}H_{42}N_2O_{17}$: C 49.56, H 6.24, N 4.13; found: C 50.65, H 6.43, N 4.86.

2,3,4-Tri-*O*-acetyl α-D-gluco-hexodialdo-1,5-pyranose-6-*O*-methyloxime (15): Compound **15** was obtained from **14** (100 mg, 0.29 mmol) through Dess–Martin oxidation in dry CH_2Cl_2 followed by reaction with *O*-methyl hydroxylamine hydrochloride in pyridine as described for the synthesis of compound **11**. Intermediate aldehyde at C-6 was not purified and final column chromatography with ethyl acetate/petroleum ether (1:1) afforded pure **15** (81 mg, 75%). $[\alpha]_D = +64.8$ ($c = 0.5$ in chloroform); ^{1}H NMR $\delta = 7.07$ (d, 1H, $J_{5,6} = 6.8$ Hz, H-6), 6.25 (d, 1H, $J_{1,2} = 3.0$ Hz; H-1), 5.45 (t, 1H, $J_{2,3} = J_{3,4} = 9.9$ Hz; H-3), 4.86 (t, 1H, $J_{3,4} = J_{4,5} = 9.6$ Hz; H-4), 4.86 (m, 1H; H-2), 4.38 (m, 1H; H-5), 3.76 ppm (s, 3H; N–OCH$_3$); ^{13}C NMR: $\delta = 141.7$, 90.8, 72.2, 71.0, 68.8, 66.6, 63.5, 54.9 ppm; MALDI-MS: m/z: 398.0 $[M+Na]^+$, 414.0 $[M+K]^+$; elemental analysis calcd (%) for C 48.00, H 5.64, N 3.73; found: C 49.11, H 5.17, N 4.32.

α- and β-D-gluco-hexodialdo-1,5-pyranose-6-*O*-methyloxime (16): Deacetylation of **15** (100 mg, 0.27 mmol) with MeONa in MeOH was carried out according to the procedure described for the preparation of **12**. Compound **16** was recovered as a 1:1 mixture of α and β anomers (55 mg, 98%). MALDI-MS: m/z: 230.4 $[M+Na]^+$, 246.8 $[M+K]^+$; elemental analysis calcd (%) for $C_7H_{13}NO_6$: C 40.58, H 6.32, N 6.76; found: C 40.32, H 5.98, N 6.09.

Methyl 6-deoxy-6-methoxyamino-6-*N*-(β-D-gluco-hexodialdo-1,5-pyrano-side-6-*O*-methyloxime)-α-D-glucopyranoside (17): Compound **16** (45 mg, 0.22 mmol) was added to a solution of **13** (50 mg, 0.22 mmol) in DMF/AcOH (2:1, 3 mL) and the mixture was stirred 6 h. Solvents were evaporated in vacuo and column chromatography of the residue with AcOEt/MeOH/water (60:40:1) afforded pure **17** (74 mg, 82%). $[\alpha]_D = +25.5$ ($c = 0.5$ in methanol); ^{1}H NMR (CD$_3$OD): $\delta = 7.28$ (d, 1H, $J_{6',5'} = 7.2$ Hz; H-6′), 4.65 (d, 1H, $J_{1,2} = 3.7$ Hz; H-1), 4.16 (d, 1H, $J_{1',2'} = 9.0$ Hz; H-1′), 3.84 (s, 3H; N–OCH$_3$), 3.75 (m, 1H; H-5), 3.74 (m, 1H; H-5′), 3.62 (s, 3H; N–OCH$_3$), 3.61 (t, 1H, $J_{2,3} = J_{3,4} = 8.9$ Hz; H-3), 3.52 (t, 1H, $J_{1',2'} = J_{2',3'} = 9.0$ Hz; H-2′), 3.44 (s, 3H; OCH$_3$), 3.44–3.36 (m, 4H; H-6a, H-3′, H-2, H-4′), 3.19 (dd, 1H, $J_{3,4} = 8.9$ Hz, $J_{4,5} = 9.6$ Hz; H-4), 3.05 ppm (dd, 1H, $J_{5,6a} = 7.3$ Hz, $J_{6a,6b} = 14.3$ Hz; H-6b); ^{13}C NMR (CD$_3$OD): $\delta = 147.6$, 100.4, 94.3, 77.7, 75.7, 73.7, 73.0, 72.3, 71.9, 70.4, 70.3, 61.3, 61.0, 55.4, 55.3 ppm; MALDI-MS: m/z: 435.8 $[M+Na]^+$, 451.4 $[M+K]^+$; elemental analysis calcd (%) for $C_{15}H_{28}N_2O_{11}$: C 43.69, H 6.84, N 6.79; found: C 44.12, H 6.11, N 6.77.

Methyl 6-deoxy-6-methoxyamino-6-*N*-(6-deoxy-6-methoxyamino-β-D-glucopyranosyl)-α-D-glucopyranoside (18): $NaCNBH_3$ (15 mg, 0.24 mmol) was added to a solution of **17** (50 mg, 0.12 mmol) in glacial AcOH (5 mL), and the mixture was stirred for 40 min. Solvents were evaporated in vacuo and column chromatography of the residue with AcOEt/MeOH/water (70:30:1) afforded pure **18** (26 mg, 53%). $[\alpha]_D = +31.2$ ($c = 0.5$ in H_2O); ^{1}H NMR (CD$_3$OD): $\delta = 4.64$ (d, 1H, $J_{1,2} = 3.8$ Hz; H-1), 3.91 (m, 2H), 3.80 (m, 1H), 3.76 (m, 1H; H-5), 3.61 (m, 1H), 3.60 (t, 1H, $J_{2,3} = J_{3,4} = 9.0$ Hz; H-3), 3.57 (s, 3H; N–OCH$_3$), 3.52 (s, 3H; N–OCH$_3$), 3.45 (s, 3H; OCH$_3$), 3.39 (dd, 1H, $J_{1,2} = 3.8$ Hz, $J_{2,3} = 9.7$ Hz; H-2), 3.23 (m, 2H; H-6′a, H-5′), 3.19 (dd, 1H, $J_{3,4} = 9.0$ Hz, $J_{4,5} = 9.7$ Hz; H-4), 3.00 (dd, 1H, $J_{5,6'b} = 5.2$ Hz, $J_{6'a,6'b} = 13.2$ Hz; H-6′b), 2.90 (dd, 1H, $J_{5,6a} = 7.1$ Hz, $J_{6a,6b} = 13.0$ Hz; H-6a), 2.84 ppm (dd, 1H, $J_{5,6a} = 8.0$ Hz, $J_{6a,6b} = 13.2$ Hz; H-6a); ^{13}C NMR (CD$_3$OD): $\delta = 100.3$, 74.8, 73.7, 74.0, 72.3, 70.9, 70.7, 69.4, 67.8, 62.3, 60.2, 60.0, 55.5, 55.2 ppm; MALDI-MS: m/z: 437.2 $[M+Na]^+$, 453.7 $[M+K]^+$; elemental analysis calcd (%) for $C_{15}H_{30}N_2O_{11}$: C 43.47, H 7.30, N 6.76; found: C 43.02, H 6.98, N 6.17.

Trisaccharide 19: Compound **16** (27 mg, 0.13 mmol) was added to a solution of **18** (36 mg, 0.087 mmol) in DMF/AcOH (1:1, 2 mL). The mixture was stirred for 12 h, after which the solvents were evaporated in vacuo. The solid residue was then dissolved in acetic anhydride/pyridine (1:2, 3 mL). The mixture was stirred for 2 h and then concentrated. Chromatography of the residue with petroleum ether/AcOEt (4:3) afforded pure **19** (41 mg, 47%). $[\alpha]_D = +78.8$ ($c = 0.6$ in chloroform); ^{1}H NMR: $\delta = 7.16$ (d, 1H, $J_{5'',6''} = 7.1$ Hz; H-6″), 5.09 (m, 1H; H-5), 5.01 (t, 1H, $J_{1',2'} = J_{2',3'} = 9.3$ Hz; H-2′), 5.40–4.80 (m, 9H; H-2″, H-3″, H-4″, H-3′, H-4′, H-1, H-2, H-3, H-4), 4.22 (d, 1H, $J_{1'',2''} = 9.3$ Hz; H-1″), 4.20 (d, 1H, $J_{1',2'} = 9.3$ Hz; H-1′), 4.01 (m, 2H; H-5′, H-5″), 3.76 (s, 3H; NOCH$_3$), 3.41 (s, 3H; NOCH$_3$), 3.38 (s, 3H; NOCH$_3$), 3.35 (s, 3H; OCH$_3$), 3.20 (dd, 1H, $J_{5,6b} = 2.5$ Hz, $J_{6a,6b} = 14.6$ Hz; H-6b), 2.92 (dd, 1H, $J_{5,6b} = 8.6$ Hz, $J_{6a,6b} = 14.6$ Hz; H-6a), 2.82 (m, 1H; H-6′a), 2.72 ppm (dd, 1H, $J_{5,6'b} = 7.3$ Hz, $J_{6'a,6'b} = 14.1$ Hz, H-6′b); ^{13}C NMR: $\delta = 145.4$, 96.85, 96.79, 92.6, 74.1, 73.5, 71.2, 71.1, 70.8, 70.5, 70.06, 70.00, 69.6, 69.3, 69.1, 67.4, 63.3, 62.3, 60.7, 60.6, 56.06, 56.03 ppm; MALDI-MS: m/z: 1005.4 $[M+Na]^+$, 1020.8 $[M+K]^+$; elemental analysis calcd (%) for $C_{40}H_{59}N_3O_{25}$: C 48.93, H 6.06, N 4.28; found: C 49.22, H 6.61, N 5.28.

Acknowledgement

We thank the EU for funding (HPRN-CT-2002–00251). J.J.-B. thanks the Ministry of Science and Technology of Spain (grant BQU2000-C1501). I.T. thanks the Scientific Grant Agency of the Ministry of Education of Slovak Republic and the Slovak Academy of Sciences (grant VEGA-2/3077/23).

[1] a) Y. C. Lee, R. T. J. Lee, *Biomol. Eng.* **1997**, *3*, 221–237; b) *Glycosciences: Status and perspectives* (Eds.: H.-J. Gabius, S. Gabius), Chapman & Hall, London, **1997**.

[2] a) J.-F. Espinosa, F. J. Cañada, J. L. Asensio, M. Martìn-Pastor, H. Dietrich, M. Martìn-Lomas, R. R. Schmidt, J. Jiménez-Barbero, *J. Am. Chem. Soc.* **1996**, *118*, 10862–10871; b) A. Wei, K. M. Boy, Y. Kishi, *J. Am. Chem. Soc.* **1995**, *117*, 9432–9436.

[3] a) W. Levy, D. Chang, *Chemistry of C-glycosides*, Elsevier, Cambridge, **1995**; b) R. U. Lemieux, S. Koto, D. Voisin, *ACS Symp. Ser.* **1979**, *87*, 17–29; c) G. R. J. Thatcher, *The Anomeric Effect and Associated Stereoelectronic Effects*, American Chemical Society, Washington DC, **1993**; d) I. Tvaroska, T. Bleha, *Adv. Carbohydr. Chem. Biochem.* **1989**, *47*, 45–103; e) A. J. Kirby, *The Anomeric Effect and Related Stereoelectronic Effects at Oxygen*, Springer, Heidelberg, Germany, **1983**.

[4] J. L. Asensio, J. F. Espinosa, H. Dietrich, F. J. Cañada, R. R. Schmidt, M. Martìn-Lomas, S. André, H.-J. Gabius, J. Jiménez-Barbero, *J. Am. Chem. Soc.* **1999**, *121*, 8995–9000.

[5] R. Ravishankar, A. Surolia, L. Vijayan, Y. Kishi, *J. Am. Chem. Soc.* **1998**, *120*, 11297–11303.

[6] J. F. Espinosa, E. Montero, A. Vian, J. L. Garcìa, J. L. Dietrich, R. R. Schmidt, M. Martin-Lomas, A. Imberty, F. J. Cañada, J. Jiménez-Barbero, *J. Am. Chem. Soc.* **1998**, *120*, 1309–1318.

[7] a) B. D. Johnston, B. M. Pinto, *J. Org. Chem.* **2000**, *65*, 4607–4617; b) G. Hummel, O. Hindsgaul, *Angew. Chem.* **1999**, *111*, 1900-1902; Angew. *Chem. Int. Ed.* **1999**, *38*, 1782–1784.

[8] H. Driguez, *ChemBioChem* **2001**, *2*, 311–318 and references therein.

[9] J. S. Andrews, T. Weimar, T. P. Frandsen, B. Svensson, B. M. Pinto, *J. Am. Chem. Soc.* **1995**, *117*, 10799–11804, and references therein.

[10] F. Schweizer, *Angew. Chem.* **2002**, *114*, 240-264; *Angew. Chem. Int. Ed.* **2002**, *41*, 230–253, and references therein.

[11] K. C. Nicolaou, H. Flörke, M. G. Egan, T. Barth, V. A. Estevez, *Tetrahedron Lett.* **1995**, *36*, 1775–1778.

[12] K. H. Jung, M. Müller, R. R. Schmidt, *Chem. Rev.* **2000**, *100*, 4423–4442.

[13] P. H. Seeberger, W.-C. Haase, *Chem. Rev.* **2000**, *100*, 4349–4393.

[14] L. A. Marcaurelle, C. R. Bertozzi, *J. Am. Chem. Soc.* **2001**, *123*, 1587–1595.

[15] E. C. Rodriguez, K. A. Winans, D. S. King, C. R. Bertozzi, *J. Am. Chem. Soc.* **1997**, *119*, 9905–9906.

[16] S. E. Cervigni, P. Dumy, M. Mutter, *Angew. Chem.* **1996**, *108*, 1325–1328; *Angew. Chem. Int. Ed.* **1996**, *35*, 1230–1232.

[17] a) P. Finch, Z. Merchant, *J. Chem. Soc. Perkin 1* **1975**, 1682–1686; b) A. Mostad, *Acta Chem. Scand.* **1978**, *32*, 733–742.
[18] F. Peri, P. Dumy, M. Mutter, *Tetrahedron* **1998**, *54*, 12269–12278.
[19] F. Peri, A. Deutman, B. La Ferla, F. Nicotra, *Chem. Commun.* **2002**, 1504–1505.
[20] a) R. U. Lemieux, A. R. Morgan, *Can. J. Chem.* **1965**, *43*, 2205–2211; b) C. L. Perrin, K. B. Armstrong, *J. Am. Chem. Soc.* **1993**, *115*, 6825–6834.
[21] J. L. Asensio, A. Garcia, M. T. Murillo, A. Fernández-Mayoralas, F. J. Cañada, C. Johnson, J. Jiménez-Barbero, *J. Am. Chem. Soc.* **1999**, *121*, 11318–11329.
[22] I. Tvaro ka, F. R. Taravel, J. P. Utille, J. P. Carver, *Carbohydr. Res.* **2002**, *337*, 353–367.
[23] I. Tvaro ka, T. Bleha, *Adv. Carbohydr. Chem. Biochem.* **1989**, *47*, 45–123.
[24] I. Tvaroška, J. P. Carver, *J. Phys. Chem.* **1996**, *100*, 11305–11313.
[25] A. Neuman, F. Longchambon, O. Abbes, H. Gillier-Pandraud, S. Perez, *Carbohydr. Res.* **1990**, *195*, 187–197.
[26] a) F. Arene, A. Neuman, F. Longchambon, *Comptes Rendues Acad. Sc. Paris* **1979**, *C288*, 331–334; b) D. C. Rohrer, A. Sarko, T. L. Bluhm, Y. N. Lee, *Acta Crystallogr.* **1980**, *36*, 650–654.
[27] N. W. H. Cheetham, P. Dasgupta, G. E. Ball, *Carbohydr. Res.* **2003**, *338*, 955–962.
[28] M. Carpintero, A. Bastida, E. Garcia-Junceda, J. Jimenez-Barbero, A. Fernandez-Mayoralas, *Eur. J. Org. Chem.* **2001**, 4127–4135.
[29] C. A. G. Haasnoot, F. A. A. M. De Leeuw, C. Altona, *Tetrahedron* **1980**, *36*, 2783–2794.
[30] a) L. Poppe, *J. Am. Chem. Soc.* **1993**, *115*, 8421–8426; b) J. L. Asensio, F. J. Cañada, J. Jiménez-Barbero, *Eur. J. Biochem.* 1995, *233*, 618–630.
[31] a) G. D. Rockwell, B. T. Grindley, *J. Am. Chem. Soc.* **1998**, *120*, 10953–10963; b) K. N. Kirschner, R. J. Woods, *Proc. Natl. Acad. Sci. USA* **2001**, *98*, 10541–10563.
[32] Jaguar 3.5, S., Inc., Portland, OR, **1998**.
[33] A. D. Becke, *J. Chem. Phys.* **1993**, *98*, 5648–5652.
[34] K. Stott, J. Stonehouse, J. Keeler, T.-L. Hwang, A. J. Shaka, *J. Am. Chem. Soc.* **1995**, *117*, 4199–4154.
[35] a) J. F. Espinosa, F. J. Cañada, J. L. Asensio, M. Martín-Pastor, H. Dietrich, M. Martín-Lomas, R. R. Schmidt, J. Jiménez-Barbero, *J. Am. Chem. Soc.* **1996**, *118*, 10862–10871; b) J. F. Espinosa, M. Bruix, O. Jarreton, T. Skrydstrup, J.-M. Beau, J. Jiménez-Barbero, *Chem. Eur. J.* **1999**, *5*, 442–448.

Received: September 30, 2003
Revised: November 18, 2003 [F5587]